ASTRONOMY & ASTROPHYSICS
SUPPLEMENT SERIES

Astron. Astrophys. Suppl. Ser. **136**, 509–514 (1999)

Stellar kinematic data for the central region of spiral galaxies. II.⋆,⋆⋆

Ph. Héraudeau[1], F. Simien[2], G. Maubon[2], and Ph. Prugniel[2]

[1] Max-Planck-Institut für Astronomie, Königstuhl 17, D-69117 Heidelberg, Germany
[2] CRAL-Observatoire de Lyon CNRS, UMR 142, F-69561 St-Genis-Laval Cedex, France

Received February 2; accepted February 17, 1999

Abstract. We present a second dataset of absorption spectroscopy on the inner region of spiral galaxies. We have determined the central velocity dispersion for 42 Sa-Sc objects and, for 32 of them, stellar rotation curves and velocity-dispersion profiles. Some of these profiles are limited to the bulge, some others do reach a region dominated by the luminosity of the disk. These data are intended to provide basic material for the study of the mass distribution and dynamical status in the central regions of spiral galaxies. Although no elaborate bulge-and-disk photometric decomposition is performed, we estimate the effects of limited resolution and contamination by disk light on the central velocity dispersion of the bulge. All the material presented in this paper, in particular the spectra, is available on-line.

Key words: galaxies: spiral — galaxies: general — galaxies: kinematics & dynamics

1. Introduction

We have recently begun to publish results on the kinematics of the stars in the inner region of spiral galaxies (Héraudeau & Simien 1998, hereafter Paper I). Our initial aim was to obtain central kinematical data on a significant sample of bright, nearby spirals with, as much as possible, available surface photometry. Here, we present the reduction of a second, more recent set of data. We have followed closely the method of Paper I at every step of the work, and only limited explanations are given in the present paper.

2. Sample and observations

Continuing the program of Paper I with the same selection criteria, we present here a sample of 42 galaxies of type Sa to Sc, both unbarred and barred, with intermediate inclination, $cz \lesssim 4000$ km s^{-1}, and absolute magnitude $-22.3 \leq M_B \leq -18.2$. Among these, 31 have surface photometry from Héraudeau & Simien (1996): hereafter HS96).

Our kinematic observations were secured at the 1.93-m telescope of the Observatoire de Haute-Provence, equipped with the CARELEC long-slit spectrograph. The selected setup provided a wavelength range of ≈ 900 Å centered on Mg b, with a pixel size of 1.8 Å and, perpendicularly to the dispersion, $1.2''$. The slit width, projected onto the plane of the sky, was $2.2''$. The instrumental dispersion was 78 km s^{-1}. We refer to Paper I for further details on the setup.

In December 1993, February and December 1994, and January 1995, a total of 10 nights of observation allowed us to collect data on the major axis of 42 galaxies. Table 2 (proposed in electronic form only) presents the log of the observations. Typically, two 45-minute exposures were obtained for each object; these exposure times were short enough to prevent the widening of the spectral lines due to flexures within the spectrograph, yet long enough to allow the measurement of kinematical parameters down to surface brightnesses of $\mu_V \simeq 21$ mag arcsec^{-2}, with an accuracy for the velocity dispersion of less than 30 km s^{-1} for most objects. For NGC 3338, a single spectrum along the minor axis was also obtained. Each night, several template stars of types ranging between G8III and K2III were observed.

As shown in Table 2, the atmospheric conditions were mediocre on average, with a seeing disk between $2''$ and

Send offprint requests to: F. Simien (simien@obs.univ-lyon1.fr)

⋆ Based on observations collected at the Observatoire de Haute-Provence.

⋆⋆ Tables 2 and 3 are presented in electronic form only; Tables 1 through 3 are available from the CDS, Strasbourg, via anonymous ftp to cdsarc.u-strasbg.fr (130.79.128.5) or via http://cdsweb.u-strasbg.fr/Abstract.html

Table 1. Catalog elements and spectroscopic results

Object	Type	α_{1950}	δ_{1950}	$B_{\rm Tc}$	D_{25}	ϵ_{25}	PA	$-M_B$	$v_{\rm hel}$	σ_0	$f_{\rm bulge}$
(1)	(2)	(3)	(4)	(5)	(6)	(7)	(8)	(9)	(10)	(11)	(12)
IC 356	Sb	04 02 34.5	+69 40 45	10.05	4.6	0.23	90	20.84	899 ± 20	145 ± 28	0.97
IC 750	Sab	11 56 17.3	+43 00 02	12.15	2.7	0.61	43	18.17	707 ± 26	118 ± 25	....
IC 2327	Sa	08 18 51.2	+03 19 45	12.80	1.3	0.68	168	19.92	2665 ± 36	115 ± 55	....
NGC 169	Sb	00 34 13.7	+23 43 00	12.31	1.9	0.57	88	21.69	4506 ± 30	176 ± 25	....
NGC 470	Sb	01 17 10.5	+03 08 53	11.85	2.8	0.45	155	20.65	2392 ± 24	145 ± 36	....
NGC 532	Sab	01 22 39.5	+09 00 18	13.28	3.7	0.69	28	19.25	2332 ± 27	125 ± 35	0.93
NGC 691	Sbc	01 47 55.8	+21 30 45	11.73	3.4	0.27	95	21.09	2646 ± 14	108 ± 23	0.99
NGC 1056	Sa	02 39 51.4	+28 21 44	12.48	2.3	0.44	160	19.22	1536 ± 08	80 ± 15	1.03
NGC 1137	Sb	02 51 26.3	+02 45 32	12.90	2.1	0.38	20	20.12	3018 ± 12	79 ± 22	0.95
NGC 1171	Sc	03 00 40.2	+43 12 11	11.82	2.7	0.57	147	21.11	2701 ± 18	83 ± 27	0.93
NGC 1186	SBbc	03 02 13.1	+42 38 33	10.65	3.2	0.63	122	22.28	2740 ± 27	137 ± 29	0.98
NGC 1343	SBb	03 32 25.2	+72 24 28	12.02	2.6	0.36	80	20.55	2201 ± 20	129 ± 20	1.02
NGC 1485	Sb	03 59 42.4	+70 51 39	11.84	2.1	0.67	22	19.40	1089 ± 09	70 ± 14	0.97
NGC 2365	SBa	07 19 23.1	+22 10 46	12.64	2.4	0.47	170	19.81	2249 ± 16	122 ± 17	0.97
NGC 2523	SBbc	08 09 14.5	+73 43 54	11.90	2.9	0.37	57	21.56	3448 ± 16	140 ± 20	....
NGC 2545	SBab	08 11 18.7	+21 30 33	12.44	2.2	0.48	170	20.85	3383 ± 13	176 ± 17	....
NGC 2726	Sa	09 01 02.8	+60 07 55	13.03	1.6	0.67	87	18.77	1554 ± 20	84 ± 25	0.93
NGC 2798	SBa	09 14 09.5	+42 12 37	12.37	2.7	0.65	160	19.62	1749 ± 22	115 ± 27	0.99
NGC 2844	Sa	09 18 38.0	+40 21 55	13.18	1.7	0.55	13	18.48	1488 ± 15	90 ± 19	0.97
NGC 2985	Sb	09 45 52.6	+72 30 44	10.49	4.7	0.27	0	21.10	1328 ± 08	150 ± 08	0.98
NGC 3021	Sbc	09 47 59.5	+33 47 20	11.98	1.4	0.42	110	19.73	1533 ± 16	59 ± 26	0.98
NGC 3041	SBc	09 50 22.5	+16 54 52	11.73	3.7	0.36	95	19.68	1438 ± 16	97 ± 30	1.01
NGC 3067	SBab	09 55 26.4	+32 36 33	12.02	2.4	0.62	105	19.60	1452 ± 17	82 ± 28	0.93
NGC 3294	Sc	10 33 23.7	+37 35 00	11.41	3.4	0.49	122	20.38	1578 ± 13	78 ± 21	0.95
NGC 3338	Sc	10 39 28.1	+14 00 34	10.78	5.7	0.40	100	20.46	1306 ± 12	91 ± 18	0.94
NGC 3368	SBab	10 44 06.9	+12 05 04	9.47	7.8	0.33	5	20.96	910 ± 09	135 ± 10	0.99
NGC 3370	Sc	10 44 23.2	+17 32 16	11.51	2.9	0.43	148	19.73	1261 ± 26	50 ± 29	0.92
NGC 3437	SBc	10 49 52.8	+23 12 01	11.35	2.6	0.68	122	19.93	1272 ± 24	108 ± 32	0.95
NGC 3810	Sc	11 38 23.5	+11 44 54	10.68	4.1	0.34	15	20.00	996 ± 10	73 ± 16	0.95
NGC 3893	SBc	11 46 01.1	+48 59 20	10.34	4.5	0.45	165	20.61	966 ± 10	111 ± 25	0.94
NGC 3898	Sab	11 46 36.3	+56 21 42	11.04	3.7	0.33	107	20.30	1153 ± 15	223 ± 18	0.99
NGC 4237	SBbc	12 14 38.2	+15 36 07	11.93	2.1	0.35	108	18.53	981 ± 12	67 ± 21	....
NGC 4380	Sab	12 22 49.6	+10 17 32	12.05	3.2	0.43	153	18.60	979 ± 10	65 ± 19	....
NGC 4698	Sa	12 45 51.8	+08 45 37	10.90	3.9	0.32	170	19.81	1026 ± 11	134 ± 19	....
NGC 4725	SBab	12 47 59.9	+25 46 19	9.46	10.4	0.31	35	21.77	1225 ± 09	145 ± 10	1.02
NGC 5364	Sbc	13 53 41.1	+05 15 33	10.50	6.3	0.31	30	20.67	1275 ± 17	95 ± 54	....
NGC 7177	SBb	21 58 18.5	+17 29 50	11.28	3.1	0.34	90	19.88	1130 ± 11	122 ± 18	0.92
NGC 7331	Sbc	22 34 47.7	+34 09 34	9.06	10.6	0.59	171	21.60	795 ± 16	150 ± 14	0.98
NGC 7606	Sb	23 16 29.2	−08 45 33	10.88	4.3	0.46	145	21.48	2187 ± 15	136 ± 23	1.02
NGC 7678	SBc	23 25 58.2	+22 08 49	11.84	2.3	0.32	5	21.58	3470 ± 21	107 ± 45	....
NGC 7814	Sab	00 00 41.1	+15 52 03	10.87	5.7	0.51	135	20.05	1035 ± 24	183 ± 21	0.98
UGC 2906	Sb	03 55 06.9	+73 56 30	13.10	2.8	0.37	5	19.72	2524 ± 34	149 ± 40	0.98

Notes. Columns (2) to (9) are from the LEDA database (status: LEDA1998); Cols. (10) to (12) are determinations of this work. Column (2): morphological type; Cols. (3), (4): coordinates; Col. (5): $B_{\rm Tc}$, integrated blue magnitude, corrected for Galactic and internal extinction; Col. (6): D_{25}, diameter at isophote $\mu_B = 25$ mag arcsec^{-2}, in arcmin; Col. (7): ϵ_{25}, ellipticity at isophote $\mu_B = 25$; Col. (8): PA, position angle of major axis, in degrees (North through East); Col. (9): M_B, absolute B magnitude, from $B_{\rm Tc}$ and kinematical distance modulus with $H_0 = 75\,{\rm km\,s^{-1}\,Mpc^{-1}}$, except for objects with a very small radial velocity (for which LEDA makes use of other parameters); Col. (10): $v_{\rm hel}$, heliocentric radial velocity, in km s^{-1}; Col. (11): σ_0, raw central velocity dispersion, in km s^{-1}, as measured in the $2.2'' \times 1.2''$ aperture; Col. (12): $f_{\rm bulge}$, factor indicating the degree to which resolution effects and contamination by disk light have influenced the observed central bulge kinematics; $\sigma_0/f_{\rm bulge}$ is then a closer approximation to the averaged, luminosity-weighted bulge velocity dispersion within $0.1r_{\rm e}$ (see Sect. 5).

3″ (FWHM) for about half the observations, 3.5″ for nine objects, and up to $\simeq$ 5.5″ in a couple of extreme cases (incidence on the reliability of the results is discussed in Sect. 6). Care has been taken to match the seeing conditions of the galaxy and star spectra, in order to ensure comparable spectroscopic resolutions.

3. Data reduction

For the reduction of the spectra, we followed closely the method used in Paper I, which was itself similar to the process used in a series of papers on early-type galaxies (Simien & Prugniel 1997a,b,c, 1998: hereafter collectively referred to as SP). We thus limit ourselves, here, to a short abstract.

As in SP and Paper I, standard pre-processing was applied to the raw data, up to the rebinning in wavelength. The galaxy centers ($r = 0$) were determined by a Gaussian fitting to a limited range ($\simeq 12''$) around the intensity peak. Compared to ellipticals, the centering was sometimes more difficult, because dust can cause strong asymmetries. In this case, and when the solution was obvious, we adopted the origin of the rotation symmetry, and we accordingly applied a correction to the r zero point. In the outer regions, cosmic-ray hits were removed with a median filter, and adjacent lines were combined with a variable weighting function (a Gaussian continuously wider faintward), by a process preserving the global fluxes. When present, emission lines were "cut" at the level of the continuum. A Fourier-Fitting technique determined the central velocity dispersion σ_0 and, when possible, the radial profile $\sigma(r)$ of the dispersion, together with the projected rotation curve $V(r)$ along the major axis. A two-pass mode (described in SP) allowed to remove cosmics on the inner lines, where the spatial resolution must be preserved.

4. On-line spectrum availability

Our spectra are available from the Hypercat extragalactic database. We have included in the Hypercat FITS Archive the raw spectra of the present sample, together with those of Paper I. This archive will be presented in full detail elsewhere, together with its scientific rationale (Maubon et al., in preparation). Here, a short overview is proposed in the Appendix; it includes preliminary information allowing to browse through the data.

5. Presentation of the results

Determinations of the heliocentric radial velocity $v_{\rm hel}$ and central velocity dispersion σ_0 are listed in Cols. (10) and (11) of Table 1. The $V(r)$ and $\sigma(r)$ profiles are presented in Fig. 1, and also in Table 3, which is available in electronic form only. Table 1 also lists (Col. 12) a factor $f_{\rm bulge}$ measuring the effects of resolution and disk-light contamination on the central velocity dispersion of the bulge; let us recall that the calculation of this factor, extensively discussed in the Appendix of Paper I, takes into account atmospheric and instrumental resolution, kinematical effect due to bulge rotation, and mixing of bulge and disk light as derived by a simple two-component model.

As in SP and Paper I, we have adopted the following convention for the position angle PA: for $0 < {\rm PA} < 180°$, $r < 0$ corresponds to the eastern side of the galaxy, for $180 < {\rm PA} < 360°$, $r < 0$ corresponds to the western side, and for ${\rm PA} = 0°$, $r < 0$ is to the North.

Tables 1, 2, and 3 are available from the CDS. The data presented here, including the graphs of Fig. 1, are also available from the Hypercat database, whose URL is given in the Appendix.

6. Discussion

We have determined the central velocity dispersion in 42 spiral galaxies. For 32 of them, we have presented profiles of the projected rotation velocity and velocity dispersion, along the major axis. The compilation of Prugniel & Simien (1996) indicates that σ_0 has been so far published for 16 of these objects, and extended kinematical profiles for only nine objects.

Together with those of Paper I, our results gather σ_0 determinations for 75 galaxies, and kinematical profiles for 64 of them; they significantly increase the limited amount already available in the literature: for all nearby spirals obeying the same selection criteria as ours, for instance, σ_0 values are so far available for less than 200 objects, and a stellar rotation curve for a few tens of them.

The accuracy of our reductions is statistically similar to that of SP; we recall that, for early-type galaxies, their kinematical measurements have contributed to the thorough study of several aspects of the Fundamental Plane (Prugniel & Simien 1994, 1996, 1997). For the present sample, direct comparison to measurements from other sources is not straightforward. Although we are able to calculate spatial resolution effects for most of our galaxies, very few other sources allow to do the same, and comparison of raw measurements is not always relevant. Let us, however, mention that for 26 galaxies in common with other works, the mean value of the raw $\Delta\sigma_0$ residuals (ours $-$ theirs) is $-10\,{\rm km\,s^{-1}}$, with a rms scatter of 22 km s^{-1}, and with no visible trend as a function of σ_0. Although marginally indicative, these small values enhance the confidence in the lack of significant systematic errors on our measurements.

For the objects observed under very poor seeing conditions, the main effect should obviously be on σ_0, but factor $f_{\rm bulge}$ provides a partial correction, and its values stay in the range $(0.92 - 1.02)$, not much wider than for the whole sample.

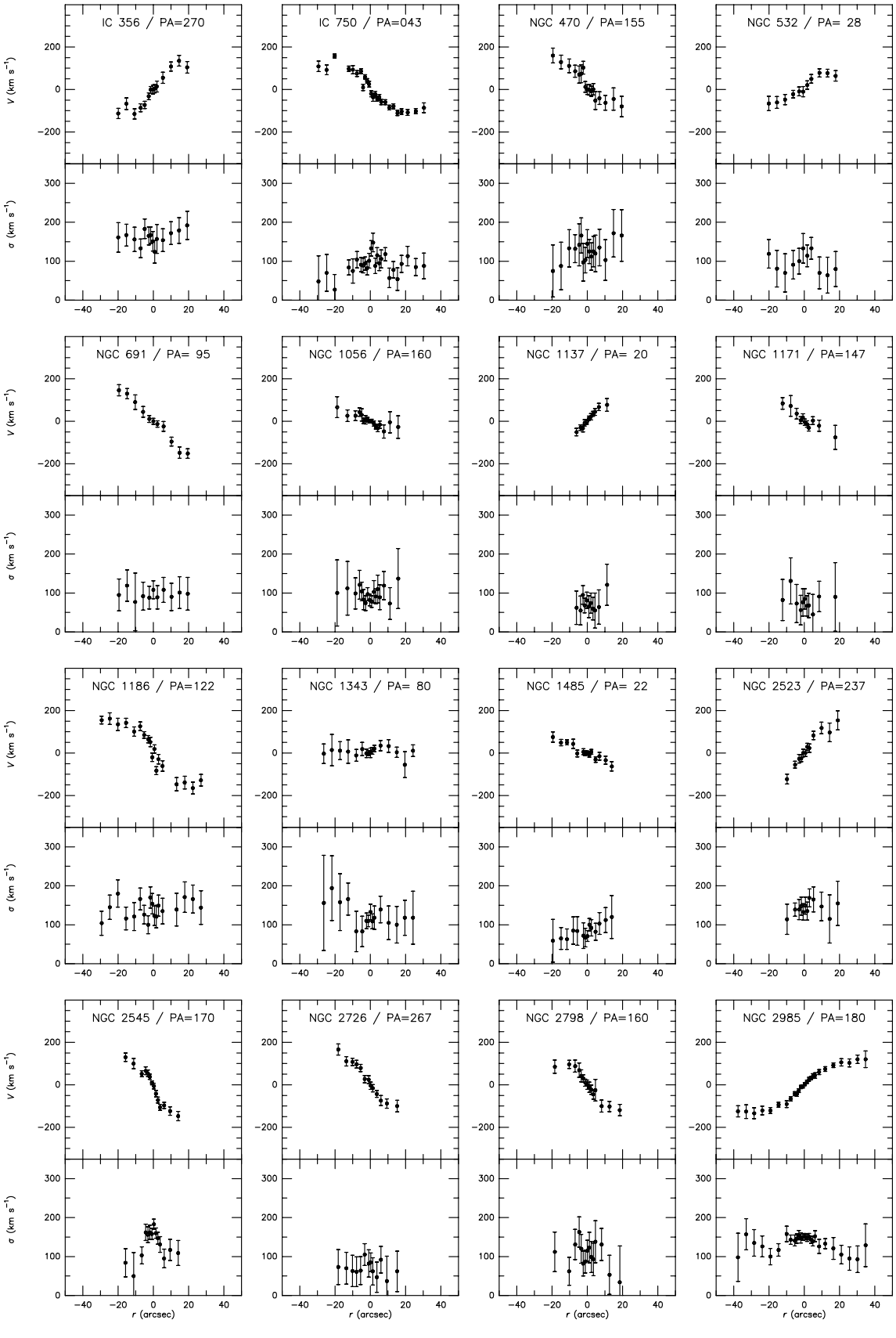

Fig. 1. Profiles of rotation velocities and velocity dispersions

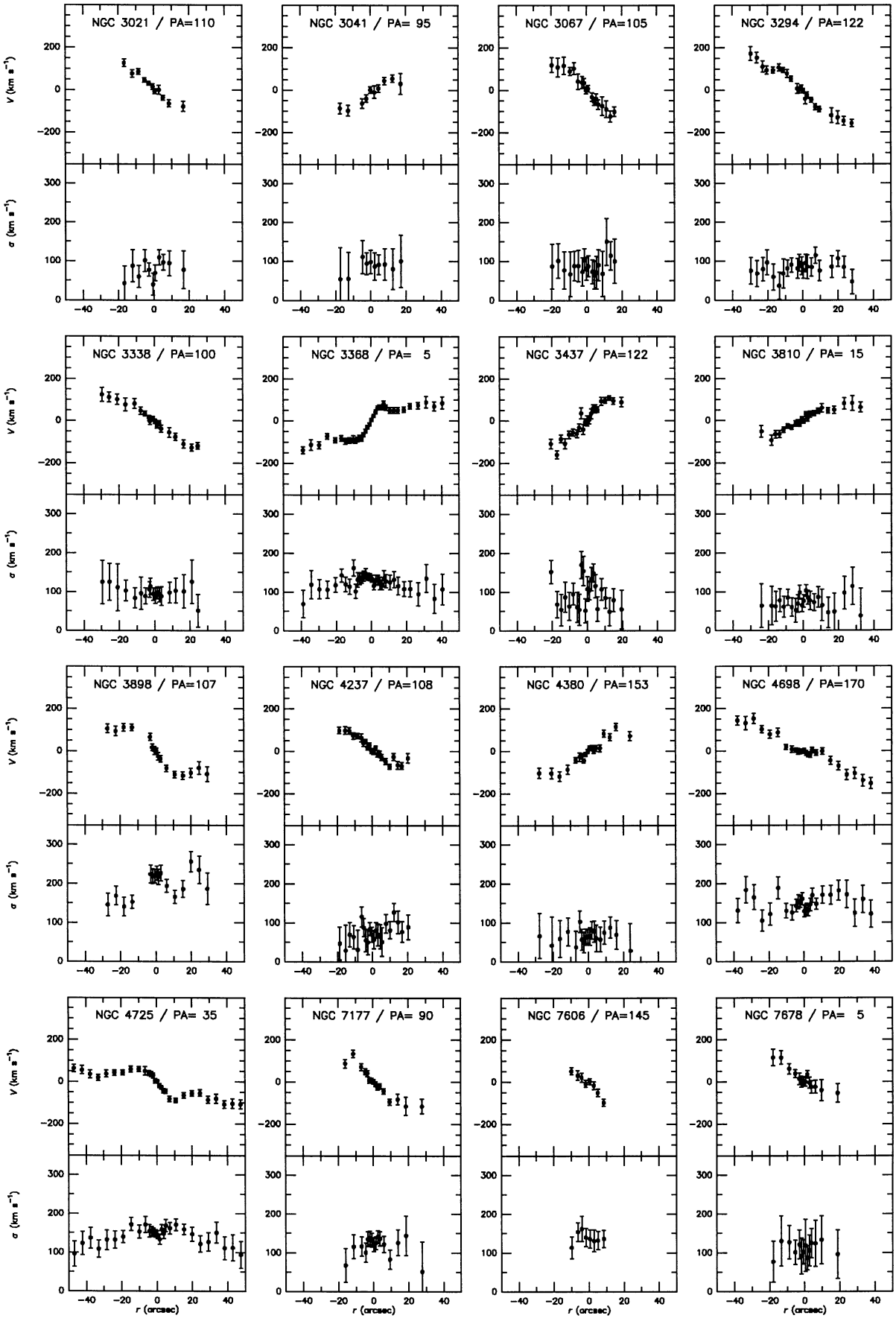

Fig. 1. continued

Our results can be used for applications involving several structural and kinematical aspects. In a forthcoming paper, we will study the mass-to-light ratios of the bulge and disk components of spirals for which surface photometry is also available.

Acknowledgements. We are indebted to the telescope operators at the Observatoire de Haute-Provence for their help in collecting the data. We thank the referee, C. Moellenhof, for his report. We have made use of the Lyon-Meudon Extragalactic Database operated by the LEDA team.

Appendix: The Hypercat FITS Archive (HFA)

The Hypercat database (Prugniel et al. 1998) has its central node at the Observatoire de Lyon, where it is accessible at `http://www-obs.univ-lyon1.fr/hypercat/`.

The FITS Archive is a newly-implemented section aimed at collecting images and spectra. We have adopted the standard of the Flexible Image Transport System because of its wide acceptance and its permanent, but controlled, evolution. A detailed on-line manual is available at `http://www-obs.univ-lyon1.fr/hypercat/11/`. Presently, the data in HFA are mostly from the Observatoire de Haute-Provence.

1) *Structure.* HFA is divided into independent datasets corresponding to material obtained in the same instrumental conditions (e.g., division by observing runs). For the spectroscopic data, the archive includes spectra of:

- scientific targets,
- template objects,
- arc lamps for wavelength calibration,
- tungsten lamps, inner dome surface or sky background, for flatfielding.

In the header of each frame, there is a set of "standard" HFA keywords which provide relevant information on the instrumental setup, conditions of observation, and the link to associated frames (e.g., nearest arc-lamp spectra, template spectra). The complete list of keywords used is available at `http://www-obs.univ-lyon1.fr/hypercat/11/keywords.html/`.

2) *Distribution.* The user can extract data from the Lyon site, or from the other two Hypercat mirrors, in Milan (Osservatorio di Brera) and Naples (Osservatorio di Capodimonte) at, respectively:
`http://palladio.brera.mi.astro.it/hypercat/`, and
`http://www.na.astro.it/hypercat/`.

3) *Evolution.* HFA is now in a stage of rapid growth. New data are appended continuously, and we will soon develop a pipeline process allowing a choice between different types of data to be extracted: options will include, e.g., flatfielding, wavelength calibration, and flux calibration. The data actually archived will be essentially the raw spectra, with the processing made at the user's request, in order to ensure homogeneous results between different sources. The following step will be the creation of higher-level procedures ("analysis pipelines") performing on-line spectrophotometric and kinematical analyses; this is planned for mid-1999.

References

Héraudeau Ph., Simien F., 1996, A&AS 118, 111 (HS96)
Héraudeau Ph., Simien F., 1998, A&AS 133, 317 (Paper I)
Prugniel Ph., Simien F., 1994, A&A 282, L1
Prugniel Ph., Simien F., 1996, A&A 309, 749
Prugniel Ph., Simien F., 1997, A&A 321, 111
Prugniel Ph., Zasov A., Busarello G., Simien F., 1998, A&AS 127, 117
Simien F., Prugniel Ph., 1997a, A&AS 122, 521
Simien F., Prugniel Ph., 1997b, A&AS 126, 15
Simien F., Prugniel Ph., 1997c, A&AS 126, 519
Simien F., Prugniel Ph., 1998, A&AS 131, 287